Dose reduction in head and neck organs through shielding and application of different scanning parameters in cone beam computed tomography: an effective dose study using an adult male anthropomorphic phantom

Diana Attaia, MMSc,[a] Stephanie Ting, MMSc,[b] Brandon Johnson, PhD,[c] Mohamed I Masoud, PhD,[d] Bernard Friedland, PhD,[e] Mona Abu El Fotouh, PhD,[f] and Shaimaa Abu el Sadat, PhD[g]

Objectives. The aim of this study was to determine the effect of shielding and scanning parameters on radiation dose reduction to the organs in the head and neck region in cone beam computed tomography (CBCT).

Study Design. An anthropomorphic phantom and optically stimulated luminescent dosimeters were used to calculate the changes in effective or equivalent doses to 9 anatomic structures through the addition of a thyroid collar, radiation safety glasses, and a radiation safety cap and by using different scanning protocols on a CS 9300 CBCT unit.

Results. The thyroid collar alone yielded dose reductions of 46% to the thyroid gland and at least 38% to the esophagus, but no more than 12% to the salivary glands. The radiation safety cap significantly reduced doses to the brain and the pituitary gland. Full shielding resulted in dose reductions of at least 50% to the thyroid gland, at least 47% to the esophagus, and approximately 35% to the brain and the pituitary gland. Significant dose reductions were recorded for all tissues with the "low dose" setting compared with the standard setting.

Conclusions. Increased protection of the organs in the head and neck regions can be achieved by using various forms of shielding in CBCT imaging, with selection of the most appropriate scanning parameters based on the purpose of the examination. (Oral Surg Oral Med Oral Pathol Oral Radiol 2020;130:101−109)

The introduction of cone beam computed tomography (CBCT) in dentistry in the early 2000s was revolutionary because it allowed for 3-dimensional (3D) evaluation of the maxillofacial region with lower effective doses compared with multidetector computed tomography (MDCT), thereby gaining wide acceptance in the profession.[1,2] CBCT is recommended for preoperative assessment of implant sites[3] because it provides more information compared with 2-dimensional (2D) imaging with regard to the relationship to vital structures and improved diagnosis for the peri-implant tissues. It also enables the fabrication of surgical stents.[4,5] The high-resolution scans afforded by CBCT are particularly important in endodontics, allowing for the evaluation of root morphology, obliterated canals, and root resorption, as well as fine details, such as dental fractures and small endodontic lesions.[6,7] CBCT also plays a role in diagnosis, treatment planning, and evaluation of progress in orthodontics, as well as the assessment of risk or complications that might be encountered. Assessment of dental structures and growth, evaluation of impacted teeth and the temporomandibular joints, pharyngeal airway analysis, and cleft lip/palate assessment are facilitated in orthodontics with CBCT.[8,9] Some criticize the use of CBCT, asserting that it does not keep radiation exposure "As Low As Reasonably Achievable" (ALARA).[10-13] However, in light of the "ALADA" (As Low As Diagnostically Acceptable) concept,[14] CBCT can be justified when it is necessary for a specific purpose.

Accordingly, questions about the health hazards and identifiable risks to patients are raised regardless of the benefits offered by CBCT.[15] Carcinogenesis, which is strongly related to the radiosensitivity of various organs and tissues, is a primary concern in oral radiology. Thus, protection of these organs and tissues is of utmost importance.[16] Organs of particular concern with regard to cancer risks include the thyroid gland, salivary glands, esophagus, and brain.[17]

Because the primary X-ray beam usually passes through the thyroid gland, the National Council on

[a]Ain Shams University Faculty of Dentistry, Cairo, Egypt.
[b]Harvard School of Dental Medicine, Boston, MA, USA.
[c]UNC Adams School of Dentistry, Chapel Hill, NC, USA.
[d]Harvard School of Dental Medicine, Boston, MA, USA.
[e]Harvard School of Dental Medicine, Boston, MA, USA.
[f]Ain Shams University Faculty of Dentistry, Cairo, Egypt.
[g]Ain Shams University Faculty of Dentistry, Cairo, Egypt.

Received for publication Jul 13, 2019; returned for revision Nov 11, 2019; accepted for publication Nov 22, 2019.

© 2019 Elsevier Inc. All rights reserved.

2212-4403/$-see front matter
https://doi.org/10.1016/j.oooo.2019.11.012

Statement of Clinical Relevance

Increased dose reduction in cone beam computed tomography for the organs in the head and neck region is achievable by using shielding in the form of a thyroid collar and radiation safety glasses and cap, along with optimizing the scanning parameters according to the purpose of the examination.

Radiation Protection and Measurements recommends using a thyroid shield whenever important landmarks would not be obscured.[18] Goren et al.,[19] Prins et al.,[20] Hidalgo et al.,[21] Qu et al.,[22] and Pauwels et al.[23] showed that shielding in the form of a thyroid collar and/or leaded eye glasses is beneficial in reducing the effective dose of CBCT to the thyroid gland and the lens of eye, thereby reducing the risk of thyroid cancer and cataracts. The radiation safety cap has been shown to have a protective effect on the head when used by clinicians in cardiology,[24,25] and yet, to the best of our knowledge, the shielding effect of this device has not been properly evaluated for dental patients.

In addition to shielding, dose reduction can be obtained by collimating the field of view (FOV) to include only the region of interest[26] and by selecting appropriate scanning parameters.[27] Today, many CBCT machines allow for the use of a low-dose scanning protocol.[28,29]

The objective of the present study was to measure the combined shielding effect of a thyroid collar, radiation safety glasses, and a radiation safety cap, along with different scanning parameters, on the thyroid gland, salivary glands, lens of the eye, bone marrow, esophagus, skin, bone surface, brain, and pituitary gland. The hypothesis was that these radiation protection measures will reduce the radiation dose to these tissues.

MATERIALS AND METHODS

Anthropomorphic phantom and dosimeters

An average adult male phantom (ATOM Max Model 711 HN; CIRS, Inc., Norfolk, VA) representing an average man, 173 cm in height and 73 kg in weight, was used in the investigation. The head and neck regions were represented by 10 slabs, each of which was 25 mm thick and contained slots corresponding to specific tissues and areas of interest both internally and externally. In total, 24 Nanodot optically stimulated luminescence dosimeters (Landauer, Glenwood, IL) were placed in the phantom as shown in Figure 1. Three sets of 24 dosimeters were barcoded and color coded for identification, with each code being assigned to a specific organ of interest corresponding to its position in the slab. The phantom was placed in a position where the plane of the slabs was approximately parallel to the floor.

Phantom preparation and shielding

An adjustable tripod was used to stabilize the phantom. The correct position was achieved by using laser beam markers and performing a scout view for each scan. The dosimeters were fixed in place by stabilizing the last slab of the phantom in the metal tray that attaches to the tripod. As a control for each of the scanning protocols, one set of dosimeters was used, and the phantom was irradiated 5 times without the use of any shielding.

OSLD ID	Organ	Slab No.
1	Calvarium Anterior	2
2	Mid Brain	2
3	Calvarium Left	3
4	Mid Brain	3
5	Calvarium Posterior	4
6	Pituitary	4
7	Right Lens of Eye	4-5
8	Left Lens of Eye	4-5
9	Right Ethmoid	5
10	Left Maxillary Sinus	6
11	Oropharyngeal Airway	7
12	Right Parotid	7
13	Left Parotid	7
14	Right Ramus	7
15	Left Ramus	7
16	Left Back of Neck	8
17	Right Submandibular Gland	8
18	Left Submandibular Gland	8
19	Center Sublingual Gland	8
20	Center C Spine	8
21	Lateral Neck – Left	9
22	Thyroid – Left	10
23	Thyroid – Right	10
24	Esophagus	10

ID: identification

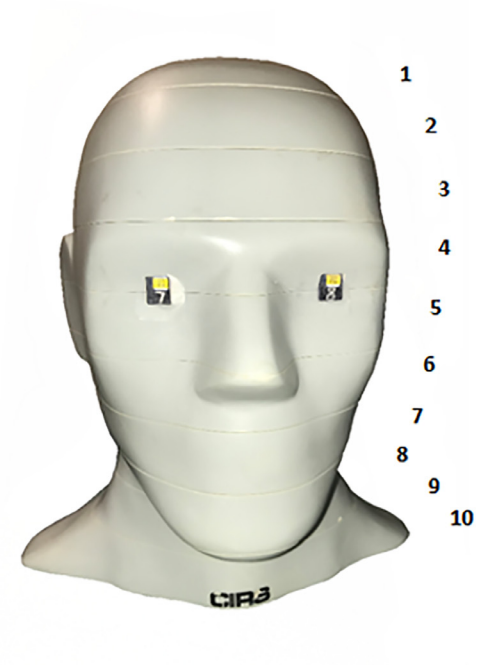

Fig. 1. Locations of optically stimulated luminescent dosimeters (OSLDs) in the ATOM adult male anthropomorphic phantom.

Fig. 2. Full shielding applied to the adult male anthropomorphic phantom during the limited field of view cone beam computed tomography scans.

When used, the shielding included a 0.5 mm lead equivalent thyroid collar (Model TC101; Penn-Jersey X-ray, Jacksonville, FL), 0.75 mm lead radiation safety glasses (Model RG-808; Phillips Safety Products, Middlesex, NJ), and a 0.5 mm lead radiation safety cap (Universal Medical, Norwood, MA) (Figure 2). For the phantom with no shielding, 1 set of dosimeters was used and exposed 5 times. For the phantom with shielding, 3 sets of dosimeters were used, and each set was exposed 5 times. Before placement of the dosimeters in the phantom for exposure, scout images were obtained to determine the proper phantom location and the exact location of the thyroid collar, glasses, and safety cap.

CBCT unit

The CS 9300 unit (Carestream Dental, Atlanta, GA) was used for the CBCT scans. The 17 × 13.5 cm FOV covered the area from nasion to menton. The 17 × 11 cm FOV was collimated to cover the area from orbitale to menton, excluding the eyes. The 10 × 10 cm FOV was confined to the dental arches. The manufacturer's default settings for the 5 scanning protocols used for an average adult, a "low dose" scanning protocol, and the shielding that was used for each protocol are shown in Table I. Each of these 5 protocols was performed 15 times, with 5 scans made for each of the 3 sets of dosimeters.

Measurement of absorbed dose

Dose measurements were done by using the dosimeters, as previously described by Ludlow et al.,[30] Johnson et al.,[31] and Goren et al.[19] Each dosimeter was kept inside a light-tight plastic container with measurements of approximately 1 × 10 × 10 mm to prevent entry of light from any source that could confound the data. A special set of Landauer MicroStar dosimeters (Landauer, Glenwood, IL) supplied by the manufacturer was used to calibrate the reader at the onset of the study. Quality assurance testing of the reader's performance was completed before each usage. Dosimeters were cleared of stored energy by using a light-emitting diode (LED) light pad before and after data recording. After approximately 24 hours, baselining of the dosimeters was completed before their next use. A scanner attached to a laptop was used to scan the barcode on each dosimeter before placing it in a portable reader.

Calculation of effective organ dose

Doses were calculated for the thyroid gland, salivary glands, lens of the eyes, bone marrow, esophagus, skin, bone surface, brain, and pituitary gland. The doses from the 15 exposures at each site were averaged. Calculation of the effective organ dose was done, as performed by Qu et al.,[32] utilizing the International Commission on Radiological Protection (ICRP) 2007 tissue-weighting factors.[33] The effective dose was the product of the tissue-weighting factor and the

Table I. Scanning protocols with different shielding

FOV (cm)	*Setting*	*Voxel size (mm)*	*kVp*	*mA*	*Exposure time (seconds)*	*Shielding*
17 × 13.5	Standard	0.3	90	4	11.30	Thyroid collar
17 × 13.5	Standard	0.5	90	4	11.30	Thyroid collar
17 × 11	Standard	0.5	90	4	6.40	Thyroid collar, radiation safety glasses, radiation safety cap
17 × 11	Low dose setting	0.4	80	2	3	Thyroid collar, radiation safety glasses, radiation safety cap
10 × 10	Standard	0.18	80	4	8	Thyroid collar

FOV, field of view; *kVp,* kilovoltage peak; *mA,* milliamperage.

equivalent dose for each weighted tissue. Because the lens of eye and the pituitary gland have no tissue weighting factors, the equivalent dose was calculated for them. Dose was expressed in microsieverts.

Scanning protocols

Comparisons between doses from scans without shielding and scans with shielding were made for all 5 protocols. Comparisons between the collimated FOV (17 × 11 cm) at the standard setting and at the "low dose" setting were performed. Comparisons between the smallest FOV scanning protocol (10 × 10 cm) at the standard setting and the other 3 scanning protocols at the standard setting were also performed.

Statistical analysis was performed by using SPSS version 16 (SPSS Inc., Chicago, IL). Microsoft Office Excel (Microsoft, Redmond, WA) was used for data handling and graphical presentation. The one sample *t* test was applied for comparing the measured results with the control. Both standard deviation and percent reductions were reported. The significance of differences in effective or equivalent doses in the 9 sites between the scans with no shielding and the scans with shielding in place was calculated, with significance established at $P < .05$.

RESULTS

The effective doses and equivalent doses for the organs are presented in Tables II to VI, with the 5 tables corresponding to the 5 exposure protocols listed in Table I. For the 17 × 13.5 cm FOV at 0.3 mm voxel size (see Table II), the thyroid collar had a significant effect ($P < .05$) in dose reduction on the thyroid gland, salivary glands, bone marrow, esophagus, and bone surface, with at least a 43% reduction in the thyroid gland and esophagus. For the same FOV at 0.5 mm voxel size (see Table III), the effect was significant ($P < .05$) for the thyroid gland, bone marrow, esophagus, and bone surface, with at least a 38% reduction in the thyroid gland and esophagus.

For the 17 × 11 cm FOV at 0.5 mm voxel size, the thyroid collar, radiation safety glasses, and radiation safety cap had a significant effect ($P < .05$) on all organs except the lens of eyes (see Table IV). For the same FOV at 0.4 mm voxel size and the "low dose" setting, the full shielding had a significant effect ($P < .05$) on the thyroid gland, bone marrow, esophagus, bone surface, brain, and the pituitary gland (see Table V). For the 17 × 11 cm FOV at both voxel sizes (see Tables IV and V), the full shielding resulted in at least a 32% dose reduction to both the brain and the pituitary gland.

For the 10 × 10 cm FOV (see Table VI), the thyroid collar alone had a significant effect ($P < .05$) on all organs except the salivary glands, brain, and the pituitary gland, yielding at least a 52% reduction to the thyroid gland and the esophagus.

Any increase in dose with the use of shielding was found to be nonsignificant ($P > .05$). As shown in Table VII, there was at least an 82.5% reduction in organ doses when using the "low dose" setting with the 17 × 11 cm FOV compared with the same FOV but with the standard setting, with the application of shielding to both protocols. Table VIII shows the percent reduction between the organ doses with the smallest FOV (10 × 10 cm) and the other 3 scanning protocols at the standard setting.

DISCUSSION

The aim of this study was to evaluate the effect of shielding and scanning parameters on the radiation doses to the organs in the head and neck region resulting from CBCT imaging. Higher doses produced by 3-D imaging as opposed to 2-D imaging are of concern.

Many studies have emphasized the effect of the thyroid collar and leaded eye glasses in reducing organ doses and total effective dose,[19,31,32] recommending their use in various scan protocols. This was reinforced

Table II. Adult male phantom full field of view at 0.3 mm voxel size

			17 × 13.5 cm Standard setting 0.3 mm voxel size			
	Without shielding	*With shielding*	*SD*	*Effect size (Cohen's d)*	*% Red.*	*P value*
Thyroid	25.4 (Eff.)	13.8* (Eff.)	4.99	58.05	46%	< .001
Salivary glands	31.8 (Eff.)	30.5† (Eff.)	50.03	2.76	4%	.041
Lens of eyes	3347 (Equi.)	3397.6 (Equi.)	65.70	0.77	−1.5%	.313
Bone marrow	14.8 (Eff.)	13.5† (Eff.)	3.40	3.14	9%	.032
Esophagus	2.8 (Eff.)	1.6* (Eff.)	1.12	26.07	43%	< .001
Skin	1.53 (Eff.)	1.51 (Eff.)	1.67	1.35	1.3%	.143
Bone surface	4.5 (Eff.)	4.2† (Eff.)	11.01	2.87	7%	.038
Brain	6.4 (Eff.)	6.7 (Eff.)	18.28	1.88	−5%	.082
Pituitary gland	1267.5 (Equi.)	1330 (Equi.)	48.31	1.29	−5%	0.155

*Highly significant difference ($P < .01$).
†Significant difference ($P < .05$).
Eff., effective dose; *Equi.,* equivalent dose; *SD,* standard deviation.

Table III. Adult male phantom Full Field of View at 0.5 mm voxel size

	17 × 13.5 cm Standard Setting 0.5 mm voxel size					
	Without shielding	*With shielding*	*SD*	*Effect Size (Cohen's d)*	*% Red.*	*P value*
Thyroid	26 (Eff.)	14* (Eff.)	1.43	214.01	46%	0.00001
Salivary glands	30.7 (Eff.)	29.1 (Eff.)	150.15	1.07	5%	0.205
Lens of eyes	3221 (Equi.)	3223.7 (Equi.)	40.47	0.05	−0.1%	0.938
Bone marrow	14.8 (Eff.)	13.5* (Eff.)	1.28	8.65	9%	0.004
Esophagus	2.6 (Eff.)	1.6* (Eff.)	0.95	26.65	38%	0.0004
Skin	1.47 (Eff.)	1.46 (Eff.)	5.75	0.21	0.7%	0.746
Bone surface	4.47 (Eff.)	4.12* (Eff.)	5.84	6.02	8%	0.009
Brain	6.3 (Eff.)	6.5 (Eff.)	13.98	1.50	−3%	0.122
Pituitary gland	1254 (Equi.)	1278.5 (Equi.)	45.58	0.54	−2%	0.449

Eff., effective dose; *Equi.,* equivalent dose; *SD,* standard deviation.
*High significant difference ($P < 0.01$).

Table V. Adult male phantom limited field of view at 0.4 mm voxel size

	17 × 11 cm "Low dose" setting 0.4 mm voxel size					
	Without shielding	*With shielding*	*SD*	*Effect size (Cohen's d)*	*% Red.*	*P value*
Thyroid	2 (Eff.)	1* (Eff.)	0.97	24.39	50%	< .001
Salivary glands	2.56 (Eff.)	2.6 (Eff.)	3.01	1.29	−1.5%	.155
Lens of eyes	133.7 (Equi.)	146.4 (Equi.)	8.22	1.55	−9.5%	.115
Bone marrow	1.33 (Eff.)	1.14† (Eff.)	0.49	3.11	14%	.032
Esophagus	0.21 (Eff.)	0.11* (Eff.)	0.15	16.44	47%	.001
Skin	0.10 (Eff.)	0.095 (Eff.)	0.35	1.18	5%	.176
Bone surface	0.44 (Eff.)	0.34* (Eff.)	1.62	6.25	23%	.008
Brain	0.44 (Eff.)	0.34† (Eff.)	3.91	3.52	32%	.025
Pituitary gland	87 (Equi.)	58† (Equi.)	6.35	4.56	33%	.015

*Highly significant difference ($P < .01$).
†Significant difference ($P < .05$).
Eff., effective dose; *Equi.,* equivalent dose; *SD,* standard deviation.

Table IV. Adult male phantom limited field of view at 0.5 mm voxel size

	17 × 11 cm Standard setting 0.5 mm voxel size					
	Without shielding	*With shielding*	*SD*	*Effect size (Cohen's d)*	*% Red.*	*P value*
Thyroid	13 (Eff.)	6.32* (Eff.)	2.74	59.53	51%	< .001
Salivary glands	17 (Eff.)	16.02† (Eff.)	49.47	2.19	6%	.062
Lens of eyes	858.7 (Equi.)	879.01 (Equi.)	55.57	0.37	-2%	.591
Bone marrow	9.1 (Eff.)	7.17* (Eff.)	1.88	8.50	21%	.004
Esophagus	1.5 (Eff.)	0.76* (Eff.)	0.53	38.28	52%	< .001
Skin	0.64 (Eff.)	0.57* (Eff.)	0.62	10.78	10%	.002
Bone surface	2.7 (Eff.)	2.14* (Eff.)	6.87	7.89	20%	.005
Brain	3.17 (Eff.)	1.95* (Eff.)	21.48	5.66	38%	.010
Pituitary gland	612 (Equi.)	386* (Equi.)	40.34	5.60	37%	.010

*Highly significant difference ($P < .01$).
†Significant difference ($P < .05$).
Eff., effective dose; *Equi.,* equivalent dose; *SD,* standard deviation.

Table VI. Adult male phantom 10 × 10 cm field of view at 0.18 mm voxel size

	10 × 10 cm Standard setting 0.18 mm voxel size					
	Without shielding	*With shielding*	*SD*	*Effect size (Cohen's d)*	*% Red.*	*P value*
Thyroid	14.26 (Eff.)	5.7* (Eff.)	7.48	28.53	60%	< .001
Salivary glands	17.16 (Eff.)	15.17 (Eff.)	104.96	1.89	12%	.081
Lens of eyes	303.8 (Equi.)	269.32† (Equi.)	8.98	3.85	11%	.021
Bone marrow	6.54 (Eff.)	5.51† (Eff.)	2.72	3.18	16%	.031
Esophagus	1.41 (Eff.)	0.67* (Eff.)	1.37	13.40	52%	.001
Skin	0.35 (Eff.)	0.31* (Eff.)	0.56	6.39	11%	.008
Bone surface	1.99 (Eff.)	1.69† (Eff.)	10.85	2.71	15%	.042
Brain	0.90 (Eff.)	0.76 (Eff.)	8.18	1.69	15%	.100
Pituitary gland	161.6 (Equi.)	137.11 (Equi.)	15.15	1.62	15%	.107

*Highly significant difference ($P < .01$).
†Significant difference ($P < .05$).
Eff., effective dose; *Equi.,* equivalent dose; *SD,* standard deviation.

Table VII. Percent reduction between the 17 × 11 cm FOV with shielding at the standard setting and at the "low dose" setting

	17 × 11 cm Standard setting 0.5 mm voxel size	*17 × 11 cm "Low dose" setting 0.4 mm voxel size*	*Percent reduction*
Thyroid	6.32 (Eff.)	1 (Eff.)	84%
Salivary glands	16.02 (Eff.)	2.6 (Eff.)	84%
Lens of eyes	879.01 (Equi.)	146.4 (Equi.)	83%
Bone marrow	7.17 (Eff.)	1.14 (Eff.)	84%
Esophagus	0.76 (Eff.)	0.11 (Eff.)	85.5%
Skin	0.57 (Eff.)	0.095 (Eff.)	83%
Bone surface	2.14 (Eff.)	0.34 (Eff.)	84%
Brain	1.95 (Eff.)	0.34 (Eff.)	82.5%
Pituitary gland	386 (Equi.)	58 (Equi.)	85%

Eff., effective dose; *Equi.,* equivalent dose; *FOV,* field of view.

Table VIII. Percent reduction between organ doses at the 10 × 10 cm FOV and the other 3 protocols at the standard setting

	10 × 10 cm Standard setting 0.18 mm voxel size	*17 × 13.5 cm Standard setting 0.3 mm voxel size*		*17 × 13.5 cm Standard setting 0.5 mm voxel size*		*17 × 11 cm Standard setting 0.5 mm voxel size*	
			Percent reduction		*Percent reduction*		*Percent reduction*
Thyroid	5.7 (Eff.)	13.8 (Eff.)	59%	14 (Eff.)	59%	6.32 (Eff.)	10%
Salivary glands	15.17 (Eff.)	30.5 (Eff.)	50%	29 (Eff.)	48%	16.02 (Eff.)	5%
Lens of eyes	269.32 (Equi.)	3397.6 (Equi.)	92%	3223.7 (Equi.)	92%	879.01 (Equi.)	69%
Bone marrow	5.51 (Eff.)	13.5 (Eff.)	59%	13.5 (Eff.)	59%	7.17 (Eff.)	23%
Esophagus	0.67 (Eff.)	1.6 (Eff.)	58%	1.6 (Eff.)	58%	0.76 (Eff.)	12%
Skin	0.31 (Eff.)	1.51 (Eff.)	79%	1.46 (Eff.)	79%	0.57 (Eff.)	46%
Bone surface	1.69 (Eff.)	4.2 (Eff.)	60%	4.12 (Eff.)	59%	2.14 (Eff.)	21%
Brain	0.76 (Eff.)	6.7 (Eff.)	89%	6.5 (Eff.)	88%	1.95 (Eff.)	61%
Pituitary gland	137.11 (Equi.)	1330 (Equi.)	90%	1278.5 (Equi.)	89%	386 (Equi.)	64%

Eff., effective dose; *Equi.,* equivalent dose.

in the present investigation. The thyroid collar was implemented independently during the 17 × 13.5 cm and 10 × 10 cm FOV acquisitions, yielding lower organ doses compared with those measured by Ludlow et al.[34] using the same CBCT machine and same FOVs, but without thyroid shielding. In comparison with the results of the study by Ludlow et al.,[34] who used the same collimated 17 × 11 cm FOV with

standard settings but with no shielding, we obtained greater than 60% dose reduction in the thyroid gland, salivary glands, bone marrow, esophagus, skin, bone surface, and brain by using full shielding in the form of a thyroid collar, radiation safety glasses, and a radiation safety cap. Lower doses to the thyroid gland and the brain were also obtained by using full shielding in comparison with those obtained by Al Najjar et al.,[35] who used no shielding for the collimated scan (maxillary−mandibular area, excluding the eyes) performed with the Iluma CBCT scanner (IMTEC, Ardmore, OK).

In the study by Qu et al.,[22] the use of the 16 × 10 cm FOV in the DCT PRO CBCT unit (Vatech, Yongin-Si, Korea) yielded higher dose results for all the organs in comparison with using the slightly larger FOV of 17 × 11 cm in the present study. Despite the use of 2 thyroid collars in the research by Qu et al., the full shielding applied for our 17 × 11 cm FOV is probably the reason for the lower results.

Goren et al.[19] used a thyroid collar as well as radiation safety glasses on a female anthropomorphic phantom exposed to a full head scan with an FOV of 17 × 23 cm and obtained effective doses of 36 μSv and 23 μSv for the thyroid gland and brain, respectively. These doses were higher than those obtained in the present study with the use of full shielding for the collimated 17 × 11 cm FOV, namely, 6.32 μSv and 1.95 μSv for those organs, respectively. Our lower results may be attributed to the smaller FOV used in this study; however, the added use of the radiation safety cap may be partially responsible for this difference in the results.

With respect to the FOV, differences were observed when comparing the exposures made with the 17 × 13.5 cm FOV at both voxel sizes and the 17 × 11 cm FOV with the smallest FOV of 10 × 10 cm at 0.18 mm voxel sizes, all of which were performed at the standard setting. We found that the use of the smallest FOV yielded the lowest organ doses, which indicates that confining the exposure to the area of interest could be of great significance in terms of dose reduction, as stated by Pauwels et al.[36]

Scanning parameters also provide a primary means to control patient dose in dental imaging. In this study, the CS 9300 was used for CBCT exposures at 90 kV. The present study revealed higher organ doses than those reported in research by Silva et al.,[37] who used the NewTom 9000 (NewTom, Imola, Bologna, Italy) and i-CAT CBCT units (Imaging Sciences International, Hatfield, PA) at 110 kV and 120 kV, respectively. Al Najjar et al.[35] used 2 CBCT units operating at 120 kVp for the full-head scans: (1) the i-CAT Platinum CBCT scanner, which yielded comparable results for the brain but a lower dose for the thyroid gland than the 17 × 13.5 cm FOV scan in our study; and (2) the Iluma CBCT unit (IMTEC, Ardmore, OK), which yielded lower results for both the brain and the thyroid gland. Even though a thyroid collar was used in our study, the lower doses reported by Silva et al. and Al Najjar et al. possibly resulted from the higher tube voltage of their scanners. This results in the production of higher energy X-ray photons, which are less attenuated by the patient's body, resulting in a lower dose.[38]

Increasing scan resolution increases image quality,[39] which is required for some dental purposes; however, this occurs at the expense of greater exposure of the patient. In the present investigation, the use of the 0.18 mm voxel size with the 10 × 10 cm FOV generated higher organ doses than those reported by Qu et al.,[17] who used a 0.4 mm voxel size with a comparable FOV. This was reinforced in our study because the organ doses obtained using the 17 × 13.5 cm FOV at 0.3 mm voxel size were higher (except for the thyroid gland) compared with those of the 17 × 13.5 cm FOV at 0.5 mm voxel size. The difference, however, was minimal.

In our study, great reductions in dose to all organs were obtained by using the "low dose" setting in the CS 9300 unit in comparison with the other four 4 protocols at standard settings. When the protocol with the "low dose" setting was compared with the same FOV with shielding but at standard settings in the present study, the changes in peak kilovoltage and milliamperage resulted in at least an 82.5% reduction in organ doses. Similarly, compared with data from the protocols at standard settings as used by Ludlow et al.[34] and Al Najjar et al.,[35] greater than a 90% reduction to all organs was obtained. An 80% reduction in doses was achieved compared with that by Qu et al.,[32] who used a NewTom 9000 CBCT scanner at standard settings with a higher tube voltage, comparable FOV, and a double thyroid collar in their study. The combined effect of using the "low dose" setting and full shielding might be responsible for this notable reduction in dose in the present investigation.

The use of the "low dose" setting in the ProMax 3-D (Planmeca, Roselle, IL) and the Picasso Trio CBCT machines (Vatech, Yongin, Republic of Korea) by Pauwels et al.[29] yielded higher dose levels than in our study for a comparable FOV, and yet doses were low enough to justify the use of that setting, when available.

In the present study, there was a nonsignificant dose increase (less than or equal to 5%) to the brain and the pituitary gland when the thyroid collar was used with the 17 × 13.5 cm FOV, and yet the dose reduction obtained in other organs by using thyroid shielding was pronounced, justifying its use. In the collimated scan, the use of the radiation safety cap resulted in a statistically significant reduction in dose to the brain and the pituitary gland. The nonsignificant increase in dose to the lens of eyes in all scanning protocols except the

10 × 10 cm FOV might have been the result of limitations in the sample size. The power analysis was appropriate, but further studies using larger sample sizes are needed for proper investigation.

The lowest effective organ doses were achieved by limiting the FOV to the area of interest, selecting the appropriate voxel size for the required purpose, adjusting the scanning parameters when possible, and using appropriate shielding. It should be noted that the results obtained in this study are applicable only to the CS 9300 CBCT unit. Further research should be conducted with other CBCT units, using various shielding and scanning parameters to confirm the importance of factors contributing to dose reduction in CBCT imaging. In addition, further investigations are needed to assess the image quality obtained by the "low dose" setting of the CS 9300 and to assess the visibility of landmarks required for the purpose of examination when the radiation safety cap is used. The effect of the radiation safety cap on children and females needs to be evaluated.

CONCLUSIONS

Increased protection of critical organs in the head and neck region and the reduction of effective or equivalent organ dose can be achieved with various forms of shielding in CBCT imaging, along with choosing the most appropriate scanning parameters based on the purpose of the examination. The use of the "low dose" setting is highly recommended, when available and when appropriate for a CBCT study.

ACKNOWLEDGMENTS

Special thanks to Dr. John Ludlow for his contribution in the study design. Statistical analysis was done by Dr. Samer Koussa, Professor of Applied Mechanics, Military Technical College, Cairo, Egypt.

FUNDING

This study was supported by the Harvard School of Dental Medicine, Boston, MA, USA, and the Faculty of Dentistry, Ain Shams University, Cairo, Egypt.

REFERENCES

1. Farrag SI. Effective dose computation for dental cone-beam CT: a comparison with MSCT and panoramic imaging. *Phys Med Biol*. 2016;6:34-39.
2. White SC, Pharoah MJ. The evolution and application of dental maxillofacial imaging modalities. *Dent Clin North Am*. 2008;52:689-705, v.
3. Tyndall DA, Price JB, Tetradis S. Position statement of the American Academy of Oral and Maxillofacial Radiology on selection criteria for the use of radiology in dental implantology with emphasis on cone beam computed tomography. *Oral Surg Oral Med Oral Pathol Oral Radiol*. 2012;113:817-826.
4. Jacobs R, Salmon B, Codari M, Hassan B, Bornstein MM. Cone beam computed tomography in implant dentistry: recommendations for clinical use. *BMC Oral Health*. 2018;18:88.
5. Almog DM, LaMar J, LaMar FR, LaMar F. Cone beam computerized tomography-based dental imaging for implant planning and surgical guidance, Part 1: Single implant in the mandibular molar region. *J Oral Implantol*. 2006;32:77-81.
6. Patel S, Brown J, Semper M, Abella F, Mannocci F. European Society of Endodontology position statement: use of cone beam computed tomography in endodontics. *Int Endod J*. 2019: 1-4.
7. Venkatesh E, Elluru SV. Cone beam computed tomography: basics and applications in dentistry. *J Istanbul Univ Fac Dent*. 2017;51:S102-S121.
8. Machado GL. CBCT imaging—a boon to orthodontics. *Saudi Dent J*. 2015;27:12-21.
9. Kapila S, Conley RS, Harrell WEJ. The current status of cone beam computed tomography imaging in orthodontics. *Dentomaxillofac Radiol*. 2011;40:24-34.
10. Suomalainen A, Pakbaznejad Esmaeili E, Robinson S. Dentomaxillofacial imaging with panoramic views and cone beam CT. *Insights Imaging*. 2015;6:1-16.
11. Okano T, Sur J. Radiation dose and protection in dentistry. *Jpn Dent Sci Rev*. 2010;46:112-121.
12. Scarfe WC. Clinical recommendations regarding use of cone beam computed tomography in orthodontic treatment. Position statement by the American Academy of Oral and Maxillofacial Radiology. *Oral Surg Oral Med Oral Pathol Oral Radiol*. 2013;116:238-257.
13. Kumar V, Ludlow J, Soares Cevidanes LH, Mol A. In vivo comparison of conventional and cone beam CT synthesized cephalograms. *Angle Orthod*. 2008;78:873-879.
14. Jaju PP, Jaju SP. Cone-beam computed tomography: time to move from ALARA to ALADA. *Imaging Sci Dent*. 2015;45:263-265.
15. Sykes JR, Lindsay R, Iball G, Thwaites DI. Dosimetry of CBCT: methods, doses and clinical consequences. *J Phys Conf Ser*. 2013;444.
16. Mallya SM, Lam EWN, Board A, et al. *White and Pharoah's Oral Radiology Principles and Interpretation*. 8th ed. St. Louis, MO: Mosby Elsevier; 2018.
17. Qu XM, Li G, Ludlow JB, Zhang ZY, Ma XC. Effective radiation dose of ProMax 3 D cone-beam computerized tomography scanner with different dental protocols. *Oral Surg Oral Med Oral Pathol Oral Radiol Endod*. 2010;110:770-776.
18. Miles DA, Langlais RP. NCRP Report No:145: Dental X-ray guidelines: their potential impact on your dental practice. *Dent Today*. 2004;23:128. 130,132 [quiz 134].
19. Goren AD, Prins RD, Dauer LT, et al. Effect of leaded glasses and thyroid shielding on cone beam CT radiation dose in an adult female phantom. *Dentomaxillofacial Radiol*. 2013;42: 20120260.
20. Prins R, Dauer LT, Colosi DC, et al. Significant reduction in dental cone beam computed tomography (CBCT) eye dose through the use of leaded glasses. *Oral Surg Oral Med Oral Pathol Oral Radiol Endod*. 2011;112:502-507.
21. Hidalgo A, Davies J, Horner K, Theodorakou C. Effectiveness of thyroid gland shielding in dental CBCT using a paediatric anthropomorphic phantom. *Dentomaxillofac Radiol*. 2015;44:20140285.
22. Qu X, Li G, Zhang Z, Ma X. Thyroid shields for radiation dose reduction during cone beam computed tomography scanning for different oral and maxillofacial regions. *Eur J Radiol*. 2012;81: e376-e380.
23. Pauwels R, Horner K, Vassileva J, Rehani MM. Thyroid shielding in cone beam computed tomography: recommendations towards appropriate use. *Dentomaxillofac Radiol*. 2019;48:20190014.

24. Kuon E, Birkel J, Schmitt M, Dahm JB. Radiation exposure benefit of a lead cap in invasive cardiology. *Heart*. 2003;89:1205-1210.
25. Durmaz E, Karadağ B, İkitimur B, et al. Effectiveness of lead cap in radiation protection of head in the cardiac catheterization laboratory. *J Am Coll Cardiol*. 2013;62:C234.
26. Lukat TD, Wong JCM, Lam EWN. Small field of view cone beam CT temporomandibular joint imaging dosimetry. *Dentomaxillofac Radiol*. 2013;42:20130082.
27. Hidalgo Rivas JA, Horner K, Thiruvenkatachari B, Davies J, Theodorakou C. Development of a low-dose protocol for cone beam CT examinations of the anterior maxilla in children. *Br J Radiol*. 2015;88:20150559.
28. Erickson R. *Assessment of Phantom Dosimetry and Image Quality of Accuitomo 170 and MiniCAT Cone-Beam Computed Tomography*. Chapel Hill, NC: University of North Carolina at Chapel Hill Graduate School; 2014.
29. Pauwels R, Beinsberger J, Collaert B, et al. Effective dose range for dental cone beam computed tomography scanners. *Eur J Radiol*. 2012;81:267-271.
30. Ludlow JB, Walker C. Assessment of phantom dosimetry and image quality of i-CAT FLX cone-beam computed tomography. *Am J Orthod Dentofac Orthop*. 2013;144:802-817.
31. Johnson KB, Ludlow JB, Mauriello SM, Platin E. Reducing the risk of intraoral radiographic imaging with collimation and thyroid shielding. *Gen Dent*. 2014;62:34-40.
32. Qu XM, Li G, Sanderink GCH, Zhang ZY, Ma XC. Dose reduction of cone beam CT scanning for the entire oral and maxillofacial regions with thyroid collars. *Dentomaxillofac Radiol*. 2012;41:373-378.
33. The 2007 Recommendations of the International Commission on Radiological Protection. ICRP publication 103. *Ann ICRP*. 2007;37:1-332.
34. Ludlow JB, Timothy R, Walker C, et al. Effective dose of dental CBCT—a meta-analysis of published data and additional data for nine CBCT units. *Dentomaxillofac Radiol*. 2015;44:20140197.
35. Al Najjar A, Colosi D, Dauer LT, et al. Comparison of adult and child radiation equivalent doses from 2 dental cone-beam computed tomography units. Am J Orthod Dentofac Orthop. 143:784-792.
36. Pauwels R, Zhang G, Theodorakou C, Walker A, Bosmans H. Effective radiation dose and eye lens dose in dental cone beam CT: effect of field of view and angle of rotation. *Br J Radiol*. 2014;87:20130654.
37. Silva MAG, Wolf U, Heinicke F, Bumann A, Visser H, Hirsch E. Cone-beam computed tomography for routine orthodontic treatment planning: a radiation dose evaluation. *Am J Orthod Dentofac Orthop*. 2008;133. 640.e1-640.e5.
38. Serman N. Production of X-rays and interactions of X-rays with matter, 2001. Available at: http://www.columbia.edu/itc/hs/dental/sophs/material/production_xrays.pdf.
39. Fakhar HB, Mallahi M, Panjnoush M, Kashani PM. Effect of voxel size and object location in the field of view on detection of bone defects in cone beam computed tomography. *J Dent (Tehran)*. 2016;13:279-286.

Reprint requests:

Diana Attaia
18 Abd El Azim El Gholmy Street
Abbas El Akkad
Nasr City
Cairo
Egypt
diana.bassem@dent.asu.edu.eg, diana.bassem.n@gmail.com